0013-7227/08/$15.00/0
Printed in U.S.A.

Endocrinology 149(12):6157–6165

doi: 10.1210/en.2008-0593

Evidence that a Protein Kinase A Substrate, Small Heat-Shock Protein 20, Modulates Myometrial Relaxation in Human Pregnancy

Elisa K. Tyson, David A. MacIntyre, Roger Smith, Eng-Cheng Chan, and Mark Read

Mothers and Babies Research Centre, The University of Newcastle, John Hunter Hospital, Newcastle 2305, Australia

For a successful human pregnancy, the phasic smooth muscle of the myometrium must remain quiescent until labor. Activation of cAMP/cAMP-dependent protein kinase A (PKA) pathways contributes to this quiescence. The small heat-shock protein 20 (HSP20) is a target of PKA, and phosphorylated HSP20 (pHSP20) modulates relaxation of tonic vascular smooth muscle via interaction with actin, independent of myosin dephosphorylation. Our objective was to determine whether relaxation in human myometrium is associated with changes in phosphorylation of HSP20. Myometrium was obtained at elective cesarean. Elevating cAMP with forskolin or rolipram (a phosphodiesterase inhibitor) caused substantial relaxation of spontaneously contracting human myometrial strips, of 92 ± 4% (mean ± SEM, n = 10) and 84 ± 7% (n = 6), respectively. Subsequent two-dimensional electrophoresis with immunoblotting of strip extracts showed a significant 2.6- and 2.1-fold increase in phosphorylated HSP20 (pHSP20) after forskolin ($P < 0.01$; n = 5) or rolipram treatment ($P < 0.05$; n = 4). Noncyclic-nucleotide-mediated relaxation, induced by the calcium channel blocker nifedipine, did not alter pHSP20. Inhibition of PKA with H89 significantly attenuated rolipram-induced relaxation ($P < 0.01$; n = 4), and partially reduced rolipram-stimulated pHSP20. Total and pHSP20 protein was unchanged in term laboring and nonlaboring myometria. Coimmunoprecipitation studies revealed a specific association of HSP20 with α-smooth muscle actin and HSP27, a key regulator of actin filament dynamics. Finally, coimmunofluorescence demonstrated moderate colocalization of HSP20 with α-smooth muscle actin in the cytoplasm of laboring myometria. Our data support a novel role for pHSP20 in the modulation of cyclic-nucleotide-mediated myometrial relaxation, through interaction with actin. pHSP20 represents an important new target for future tocolytic therapy. (*Endocrinology* 149: 6157–6165, 2008)

OUR KNOWLEDGE OF the biochemical and mechanical events of contraction/relaxation has focused on the thick filament myosin. These well characterized changes in calcium-dependent phosphorylation/dephosphorylation of myosin light chains (MLCs) can be modified by other pathways. Alteration of the actin filament may also modulate force generation. Mechanisms include the extent of actin polymerization, with dynamic changes in filamentous actin (F-actin) to globular actin ratio or inhibition of binding of phosphorylated myosin (1–3). Inhibition of actin polymerization, independent of calcium concentration or MLC phosphorylation, attenuates force development in several smooth muscles (1, 3–5), including rat myometrium (6). Throughout much of gestation, the myometrium remains quiescent, accommodating the growing fetus. A major signaling pathway implicated in maintaining myometrial relaxation is the cAMP/cAMP-dependent protein kinase A (PKA) pathway (7); however, its substrates are poorly defined, as sustained cyclic-nucleotide-induced relaxation may occur without MLC dephosphorylation or with fixed calcium concentration (8–10). In vascular muscle, a key PKA target is the small heat-shock protein 20 (HSP20), which may actively regulate the actin filament (11).

HSP20 is abundantly expressed in all muscles (12) and belongs to the small heat-shock protein (sHSP) family. Mammalian sHSPs share several properties, including the ability to form large molecular weight homo- and hetero-oligomeric intracellular complexes (13). Phosphorylation causes dissociation of these hetero-oligomeric complexes, thereby critically regulating the function of sHSPs allowing interaction of smaller phosphorylated dimers/oligomers with their targets (14, 15). HSP20 and another sHSP, HSP27, have been implicated in the modulation of contraction and relaxation. Increasing evidence suggests phosphorylated HSP27 mediates smooth muscle contraction, through interaction with and stabilization of actin filaments (16, 17). We recently reported increases in a specific HSP27 phospho-isoform at human labor, together with a relocation of HSP27 to the actin cytoskeleton (18). Conversely, it is hypothesized that phosphorylated HSP20 (pHSP20) is an effector of cyclic-nucleotide-mediated relaxation in vascular muscle.

HSP20 is phosphorylated at serine-16 (19, 20) during cyclic-nucleotide-induced relaxation of precontracted arteries, independent of MLC phosphorylation (19, 21, 22). Early observations that term umbilical arteries were uniquely refractory to cyclic-nucleotide-mediated relaxation, coincident with failure of cAMP/cGMP activation to increase HSP20 phosphorylation in these vessels, suggested a direct role for pHSP20 in smooth muscle relaxation (23, 24). Furthermore,

First Published Online August 28, 2008

Abbreviations: 1D, One-dimensional; 2D, two-dimensional; F-actin, filamentous actin; HSP20, heat-shock protein 20; IP, immunoprecipitated; L, laboring; MLC, myosin light chain; NL, nonlaboring; PDE, phosphodiesterase; pHSP20, phosphorylated HSP20; pI, isoelectric point; PKA, protein kinase A; sHSP, small HSP; α-SMA, α-smooth muscle actin.

***Endocrinology* is published monthly by The Endocrine Society (http://www.endo-society.org), the foremost professional society serving the endocrine community.**

application of a phosphopeptide HSP20 analog, containing phospho-serine-16, to permeabilized arteries inhibited agonist-stimulated contraction, whereas an unphosphorylated peptide had no effect (20). Similarly, a transducible HSP20 phosphopeptide relaxed several types of precontracted vessels (25, 26) and caused cytoskeletal disruption in fibroblasts (27). Transducible phosphorylated full-length recombinant HSP20 also inhibited 5-hydroxytryptamine-induced contraction of umbilical arteries (28). Thus, pHSP20 promotes cyclic-nucleotide-induced relaxation of tonic vascular muscle.

The role of pHSP20 in phasic myometrial smooth muscle is unknown. A single study has identified HSP20 in rat myometrium; mRNA and protein were highly expressed in early and midgestation, with a significant decline in late gestation and labor (29). Coupled with evidence that pHSP20 may mediate vascular muscle relaxation, these findings suggest HSP20 contributes to myometrial quiescence and may modulate myometrial relaxation through interaction with actin. pHSP20 may therefore provide a novel target for manipulating myometrial relaxation.

Our studies sought to determine HSP20 expression in term laboring (L) and nonlaboring (NL) human myometrium, and to examine HSP20 phosphorylation during myometrial relaxation. We hypothesized that 1) stimulation of cAMP/PKA pathways induces HSP20 phosphorylation and myometrial relaxation; 2) nifedipine, as an agent causing noncyclic-nucleotide-mediated relaxation, does not increase pHSP20; 3) agonist-induced increases in pHSP20 are attenuated by PKA inhibitor H89; and 4) pHSP20 is lower in L than NL myometria. Finally, we hypothesized the binding partners of HSP20 in myometrium include actin and HSP27.

Materials and Methods

Subjects

All experiments performed were approved by the Hunter Area Research Committee, adhering to guidelines of the University of Newcastle and John Hunter Hospital, Newcastle, Australia, and the KK Women's and Children's Hospital, Singapore. Human myometrial samples (5 × 5 × 10 mm) were obtained from the lower uterine segment of term singleton pregnancies (gestation 38 wk, 4 d ± 1 d, mean ± SEM). After biopsy, samples were dissected from connective tissue and frozen in liquid nitrogen or placed into ice-cold saline and stored at 4 C (maximum 16 h) for contractility studies. NL cesarean sections were performed for previous section (n = 25), breech (n = 14), placenta praevia (n = 5), uterine fibroid (n = 1), ovarian mass (n = 1), and cervical septum (n = 1). During L, sections were performed for breech (n = 3), cephalopelvic disproportion (n = 3), poor progression (n = 3), and fetal distress (n = 1). All experiments performed used NL myometrial samples, unless otherwise stated.

Isometric tension recordings

Samples were cut into strips (7 × 2 × 2 mm) and suspended in organ baths containing 15 ml Krebs-Henseleit buffer with 1.89 mM $CaCl_2$. Strips were connected to a Grass FT03C force transducer (Grass Instruments, Quincy, MA) and 1 g passive tension applied. Buffer was replaced five times during the first hour. Strips were maintained at 37 C (pH 7.4) and continuously bubbled with 95% O_2/5% CO_2. Strips were equilibrated another 60–90 min, until spontaneous contractions developed. Data were digitized using a Maclab8E data-acquisition system and analyzed using Chart software (ADI, Melbourne, Australia). Contractility was measured as integrated area under the tension-time curve. Response was reported as a percentage of spontaneous baseline activity before treatment. Strips were exposed to cumulative doses of drug at approximately 20-min intervals and then frozen in liquid N_2 for protein studies. Drugs (forskolin, rolipram, nifedipine, and H89) were obtained from Sigma-Aldrich (St. Louis, MO). Untreated and vehicle controls were included in each experiment. Curves were compared by nonlinear regression analysis and EC_{50} calculated using GraphPad Prism (San Diego, CA).

One-dimensional (1D) SDS-PAGE

After pulverization under liquid N_2, 100 mg tissue was homogenized in 1 ml lysis buffer (7 M urea, 2 M thiourea, 4% CHAPS, 30 mM Tris) supplemented with phosphatase inhibitors 0.5 M EGTA, and 0.1 M Na_3VO_4. The homogenate was centrifuged (11,000 × *g*, for 15 min at 4 C) and protein determined by 2D Quant Kit (GE Healthcare, Piscataway, NJ). To assess total HSP20, 1D SDS-PAGE was performed. Reagents and equipment were obtained from Invitrogen (Mt. Waverley, Australia), unless stated otherwise. NL or L extracts (10 μg) were loaded onto 10% NuPAGE gels and separated using a Novex Mini-Cell system, at constant voltage (160 V for 80 min).

Two-dimensional (2D) SDS-PAGE

HSP20 phosphorylation was assessed using 2D-gel electrophoresis with immunoblotting. Protein (20 μg) was combined with 20 mM dithiothreitol (Bio-Rad Laboratories, Hercules, CA) and rehydration buffer (8 M urea, 2% CHAPS, 0.5% ampholytes, 0.002% bromophenol blue) made up to 155 μl. After centrifugation (11,000 × *g* for 5 min), extracts were applied to pH gradient gel strips (7.7 cm, pH 3–10 nonlinear) and rehydrated overnight. Isoelectric focusing was performed as follows: 200 V for 15 min, 450 V for 15 min, ramp at 1500 V and then 2000 V for 75 min. Gel strips were equilibrated in 5 ml lithium dodecyl sulfate sample buffer with 0.5 ml sample reducing agent at room temperature (Invitrogen) and then with 125 mM iodoacetamide (Sigma-Aldrich). Proteins were separated on 4–12% ZOOM gels.

Immunoblotting

After 1D or 2D SDS-PAGE, proteins were transferred to Hybond-C nitrocellulose (Amersham Biosciences, Buckinghamshire, UK) using the XCell II Blot Module (Invitrogen). Membranes were blocked in 5% skim milk in TBS/T (500 mM NaCl, 20 mM Tris, 0.01% Tween 20) for 2 h and incubated with total HSP20 antibody (1:7000; catalog item 07-490; Upstate Cell Signaling, Lake Placid, NY) for 2 h in 5% skim milk/TBS/T at room temperature. Blots were washed five times in TBS/T and incubated with antirabbit horseradish peroxidase conjugate (1:10,000; Santa Cruz Biotechnology, Santa Cruz, CA) for 1 h. Immunoreactive products were detected with enhanced chemiluminescence (ECL Western blotting reagents; GE Biosciences, Buckinghamshire, UK) and visualized using the Fuji Intelligent Dark Box LAS-3000 Image Reader (Fuji Photo Film, Tokyo, Japan). Densitometric analysis of specific immunoreactive protein spots (obtained after 2D SDS-PAGE) was performed using Multigauge software (Fuji Photo Film) supplied with the LAS-3000. OD (arbitrary units) of each spot was expressed as a percentage of total density of both protein spots. Percentages of the more acidic spot (representing pHSP20) were compared between control samples and matched treated samples. Similarly, densitometry was performed for the specific band obtained after 1D SDS-PAGE. For 1D gels, membranes were reprobed with α-smooth muscle actin (α-SMA) (1:7500; Sigma-Aldrich; catalog item A2547) as loading control. A pooled control of myometrial protein was included on each gel, to minimize inter-gel variation. Student's paired *t* tests or ANOVA for multiple comparisons with Tukey-Kramer test were performed as appropriate (GraphPad InstatV3, San Diego, CA). Significance was accepted for $P < 0.05$.

Coimmunoprecipitation

Protein was extracted from NL samples frozen immediately after cesarean or from NL strips after contractility studies. Crushed tissue (100 mg) was homogenized in 1 ml lysis buffer (150 mM NaCl, 0.5% Nonidet P-40, 50 mM Tris HCl, 5 mM EDTA) and centrifuged (11,000 × *g* for 15 min). Protein (50 μg) was combined with 1 μg HSP20 antibody and incubated overnight (4 C). Twenty microliters of protein A-coupled Sepharose beads (Santa Cruz Biotechnology) were incubated with the protein/antibody mixture (4 h at 4 C) and then centrifuged (400 × *g* for 5 min). The pellet was washed three times with lysis buffer and resus-

pended in 60 μl lithium dodecyl sulfate loading buffer (Invitrogen). The mixture was boiled for 10 min, centrifuged (11,000 × *g* for 3 min), and supernatant collected. Extracts (20 μl) were resolved by 1D SDS-PAGE and transferred to nitrocellulose. Immunoblotting was performed with HSP20, HSP27 (1:3000; catalog item 06-478; Upstate Cell Signaling), and α-SMA (1:7500) antibodies. Negative controls of pooled myometrial extracts, protein A-Sepharose beads, and normal goat IgG antibody (Santa Cruz Biotechnology) substituted for HSP20 antibody were included.

Immunofluorescence microscopy

Immunofluorescence was performed as previously described (18). Briefly, myometria obtained at cesarean (n = 5 for NL and L) were fixed in neutral-buffered formalin and embedded in paraffin. After antigen retrieval, 10-μm sections were blocked in 10% fetal calf serum in PBS for 30 min and then incubated with HSP20 (1:400) and α-SMA (1:500) antibodies diluted in blocking buffer for 1 h. Slides were rinsed three times for 5 min with PBS and incubated with Alexa Fluor 488 goat antimouse IgG and Alexa Fluor 594 goat antirabbit IgG (Invitrogen; both at 1:2000) as secondary antibodies. 4′,6-Diamidino-2-phenylindole (1:333) was used to stain the nuclei. As controls, sections were incubated with preimmune sera and secondary antibodies alone to determine immunoreactive specificity. Sections were then washed in PBS and mounted onto slides with Vectashield H-100 (Vector Labs, Peterborough, UK). Sections were viewed using a Zeiss Axiocam MRm(v2) and Axioplan 2 epifluorescent microscope (Carl Zeiss, Sydney, Australia). Image registration was calibrated using a Focalcheck Fluorescence Microscope Test Slide (no. 1; Molecular Probes, Invitrogen). Analyses were performed using the Colocalization Module of the Axiovision software package to derive colocalization masks. A scatterplot of intensity values was created using measured channel values for each pixel. A threshold pixel was defined such that pixel intensity values for each channel must both exceed a particular value; this was then recorded as a colocalized pixel. The colocalized pixels were highlighted as a mask.

Results

Activation of cAMP/PKA-dependent pathways results in myometrial relaxation

Because HSP20 is a cAMP/PKA substrate in vascular muscle, myometrial tension after treatment with agents elevating cAMP was examined (Fig. 1, A and B). Forskolin, an adenylate cyclase activator, and rolipram, a specific phosphodiesterase (PDE) type 4B inhibitor, caused similar maximal reduction in contractility of 92 ± 4% (n = 10–13) and 84 ± 7% (n = 6–10), respectively (mean ± SEM) (Fig. 1E). Complete

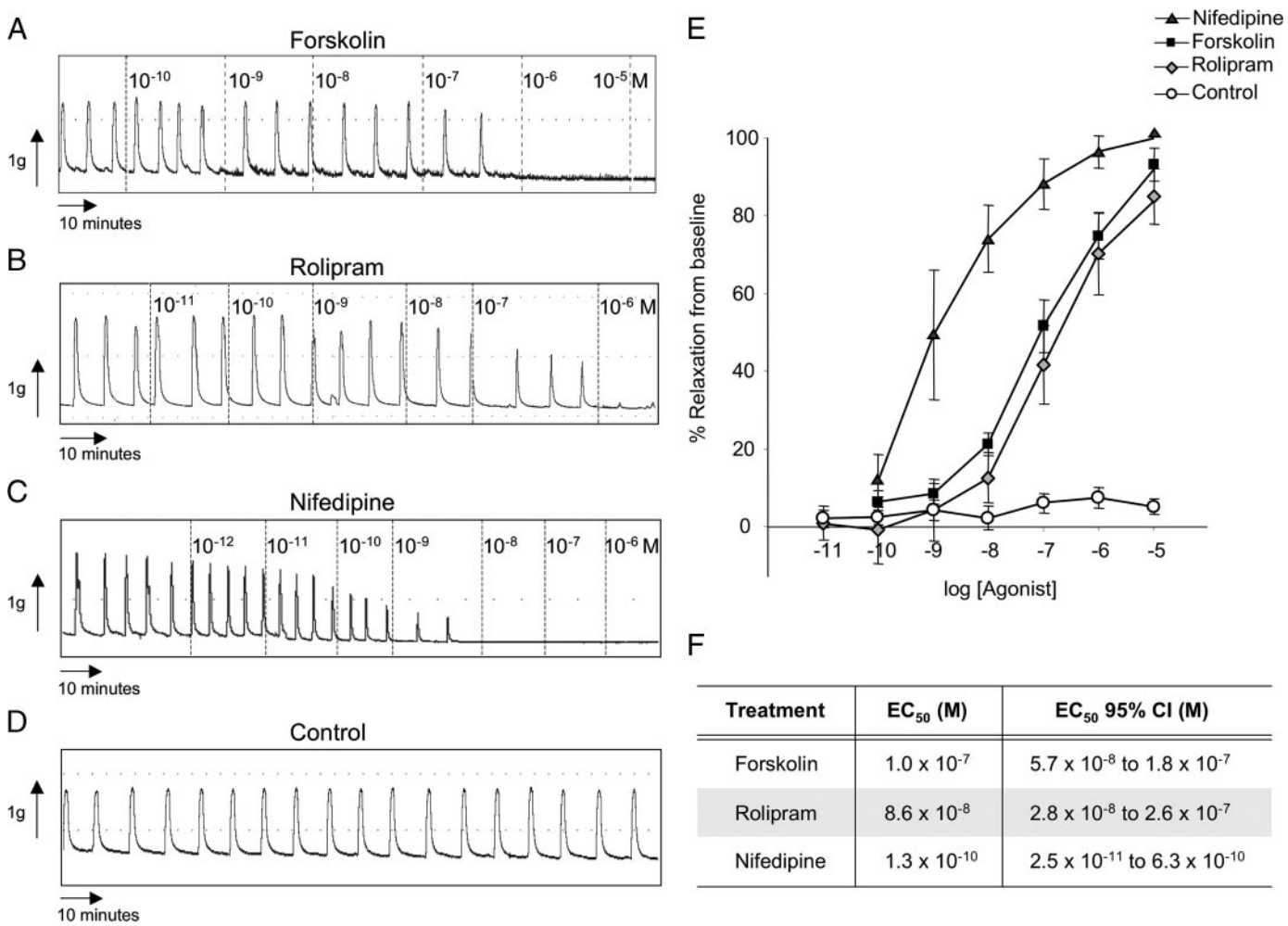

F

Treatment	EC_{50} (M)	EC_{50} 95% CI (M)
Forskolin	1.0×10^{-7}	5.7×10^{-8} to 1.8×10^{-7}
Rolipram	8.6×10^{-8}	2.8×10^{-8} to 2.6×10^{-7}
Nifedipine	1.3×10^{-10}	2.5×10^{-11} to 6.3×10^{-10}

FIG. 1. Agonist-induced inhibition of myometrial contractility. A–D, Representative isometric tension recordings of spontaneous contractions in human myometrial strips after cumulative doses of forskolin 10^{-10} to 10^{-5} M (A), rolipram 10^{-11} to 10^{-6} M (B), or nifedipine 10^{-12} to 10^{-6} M (C) or untreated control (D). Tension generated is represented in grams, with time in minutes. E, Cumulative effect of agonist on contractile activity. Relaxation responses to treatment were compared as a percentage of basal spontaneous activity before treatment. Data points represent the mean ± SEM. Relaxation measured as integrated area under the tension curve. F, EC_{50} calculated after fitting of idealized dose-response curves using GraphPad Prism software. Forskolin, n = 10–13; rolipram, n = 6–10; nifedipine, n = 5; and controls, n = 10.

inhibition of contraction was defined as 100% relaxation. PDE type 4, the most abundant PDE isoform at term, is selective for cAMP (30). Therefore, rolipram potentiates cAMP by inhibiting its breakdown. In control strips, there was no change in tension, with a 5 ± 2% (n = 10) reduction from baseline at experiment conclusion (Fig. 1E).

To examine HSP20 phosphorylation in noncyclic-nucleotide-mediated relaxation, the effects of the Ca^{2+}-channel blocker nifedipine were studied. Nifedipine caused 100% relaxation in all strips (n = 5) (Fig. 1C). The EC_{50} of nifedipine was significantly lower than forskolin and rolipram (Fig. 1F), indicating the enhanced potency of nifedipine.

Activation of cAMP/PKA-dependent pathways results in increased HSP20 phosphorylation

To determine whether HSP20 is phosphorylated in human myometrium during cAMP-mediated relaxation, protein was extracted from strips treated with forskolin or rolipram and from matched control strips. 2D SDS-PAGE and immunoblotting with total HSP20 antibody was performed. This allowed detection of unphosphorylated and phosphorylated HSP20 isoforms, because the additional phosphate group increases protein acidity (Fig. 2). Two specific immunoreactive spots were seen: a basic spot at isoelectric point (pI) of approximately 6.3 (representing unphosphorylated HSP20), and a more acidic spot at pI approximately 5.9 (representing pHSP20), consistent with published data (20, 22). Forskolin- and rolipram-induced relaxation caused a shift of HSP20 isoforms, with an increase in pHSP20 and concurrent decrease in unphosphorylated HSP20, compared with matched controls (Fig. 2, A and B). The OD of each spot was expressed as a percentage of the total density of both protein spots. Densitometry revealed forskolin significantly increased pHSP20, from 16 ± 2% (n = 5) in control strips to 42 ± 4% (mean ± SEM, n = 5; $P < 0.01$, Student's paired *t* test) (Fig. 2D). There was no change in total HSP20 expression after treatment, as assessed by 1D SDS-PAGE and immunoblotting (data not shown). Rolipram treatment of strips also

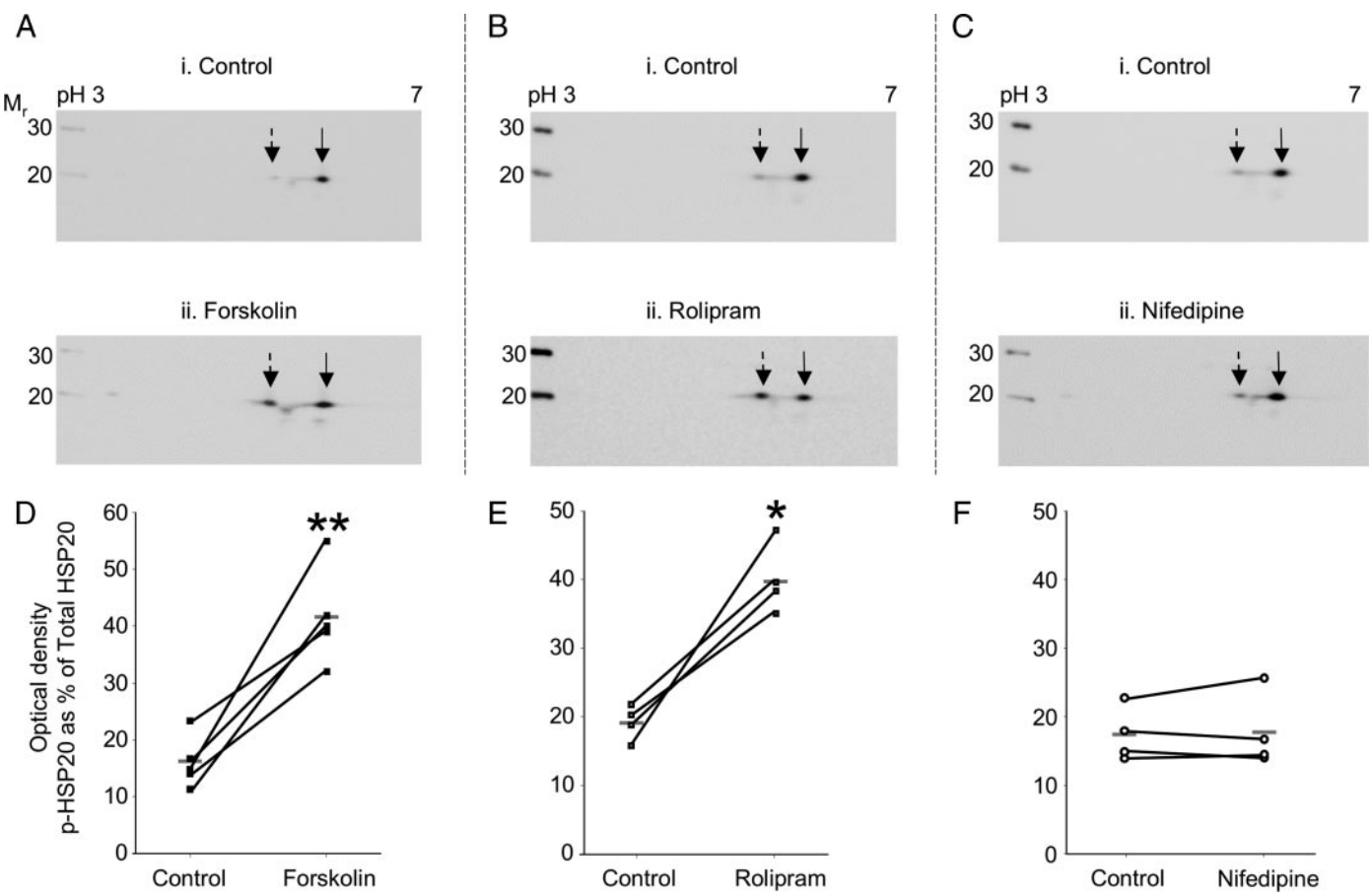

FIG. 2. Changes in phosphorylation of HSP20 during cAMP- and non-cAMP-mediated relaxation of spontaneously contracting myometrial strips. Representative 2D immunoblots of myometrial strips treated with cumulative doses of forskolin 10^{-10} to 10^{-5} M (n = 5) (A), rolipram 10^{-11} to 10^{-6} M (n = 4) (B), or nifedipine 10^{-11} to 10^{-6} M (n = 4) (C), each with respective matched control. Protein (20 μg) was extracted from strips, resolved by 2D SDS-PAGE, transferred to nitrocellulose, and probed with anti-total HSP20. There was an increase in pHSP20 (*dashed arrow*) after forskolin (A) or rolipram (B) treatment compared with untreated matched control strips. Densitometric analysis revealed HSP20 phosphorylation was significantly increased after treatment with forskolin (D) or rolipram (E) (**, $P < 0.01$; *, $P < 0.05$, compared with matched control), whereas HSP20 phosphorylation was unchanged after treatment with nifedipine (F). C and F, Individual data points for each muscle strip shown. Density of immunoreactive protein spots is expressed as a percentage of the total density of both spots. The more acidic spot represents pHSP20 (*dotted arrow*), whereas the more basic spot represents unphosphorylated HSP20 (*black arrow*). M_r, Relative molecular mass × 1000; pH gradient along the *top of panel*.

increased HSP20 phosphorylation, from 19 ± 2% in controls to 40 ± 3% (n = 4; $P < 0.05$) (Fig. 2E). Vehicle (ethanol) controls showed no change in pHSP20 levels; pHSP20 was 19 ± 2% (n = 3) in matched controls and 20 ± 4% (n = 3) after ethanol (data not shown).

To examine HSP20 phosphorylation in noncyclic-nucleotide-mediated relaxation, the effects of nifedipine were studied. Immunoblotting of protein from nifedipine-treated strips demonstrated no change in pHSP20 (Fig. 2C). pHSP20 in matched controls was 17 ± 2% and was unchanged at 18 ± 3% after nifedipine (n = 4) (Fig. 2F).

PKA inhibitor H89 reduces rolipram-induced myometrial relaxation

To determine the role of PKA in HSP20 phosphorylation in human myometrium, the effects of the selective PKA inhibitor H89 on cAMP-mediated relaxation were examined. In a separate set of experiments, contractile responses to rolipram were assessed in the presence and absence of H89 (Fig. 3, A–C). Rolipram alone elicited an 82 ± 13% (n = 4) reduction in contractility. In matched samples pretreated with H89, rolipram was less efficacious, causing a 57 ± 11% (n = 4) reduction in contractility (Fig. 3D) with a significant shift of the dose-response curve ($P < 0.01$, ANOVA). The potency of rolipram was unchanged by H89 (Fig. 3E). H89 10^{-5} M alone exerted no significant change from baseline contractility, with 2 ± 6% reduction (mean ± SEM, n = 8; data not shown).

Rolipram-induced HSP20 phosphorylation is partially reduced by H89 pretreatment

We hypothesized that H89-meditated PKA inhibition reduces agonist-induced HSP20 phosphorylation in myometrial smooth muscle. Protein was extracted from strips treated with rolipram alone or rolipram with H89 pretreatment. Immunoblotting after 2D SDS-PAGE revealed an increase in pHSP20 abundance after rolipram 10^{-11} to 10^{-6} M, compared with untreated matched controls (Fig. 4A). With H89 10^{-5} M treatment before rolipram 10^{-11} to 10^{-6} M, the increase in pHSP20 induced by rolipram was attenuated (Fig. 4A). pHSP20 was 17 ± 4% in controls, with a significant increase after rolipram alone to 39 ± 6% ($P < 0.01$, ANOVA; n = 4). Rolipram in the presence of H89 caused a smaller increase in HSP20 phosphorylation, achieving a mean level of 31 ± 3% ($P < 0.05$ *vs.* matched controls; n = 4) (Fig. 4B). Although there was a trend toward reduced rolipram-stimulated HSP20 phosphorylation by H89, levels of HSP20 phosphorylation attained were not statistically different in the presence or absence of H89 (ANOVA with Tukey-Kramer test).

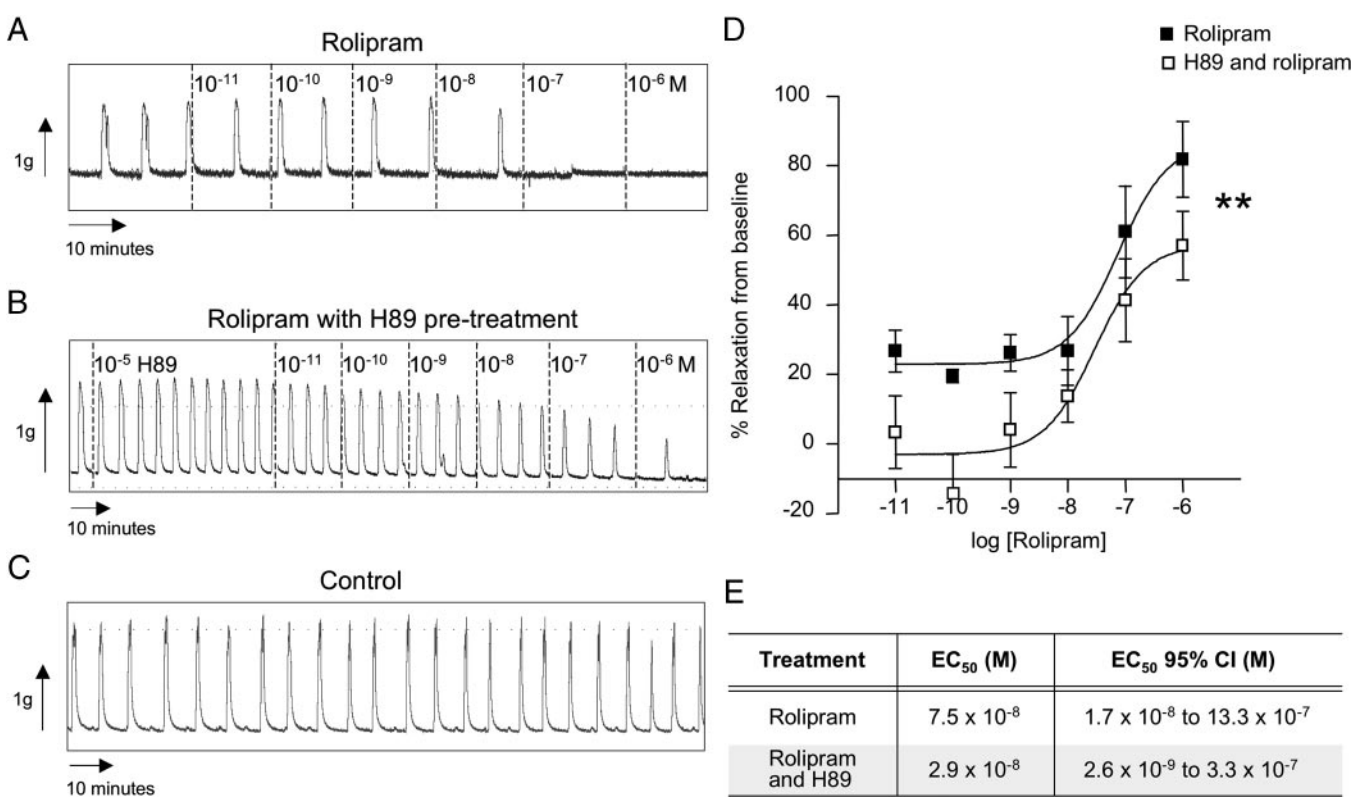

E

Treatment	EC_{50} (M)	EC_{50} 95% CI (M)
Rolipram	7.5×10^{-8}	1.7×10^{-8} to 13.3×10^{-7}
Rolipram and H89	2.9×10^{-8}	2.6×10^{-9} to 3.3×10^{-7}

FIG. 3. Rolipram-induced relaxation of myometrial strips in the presence and absence of H89. A–C, Original isometric tension recordings of spontaneous contractions in human myometrial strips after treatment with rolipram 10^{-11} to 10^{-6} M (A) or H89 10^{-5} M (B), pretreatment for 60 min, and then rolipram 10^{-11} to 10^{-6} M or control (C). Contractile activity was maximally reduced after rolipram alone. D, Cumulative effect of agonist on contractile activity. Relaxation responses to treatment were compared as a percentage of basal spontaneous activity. Rolipram was less effective in the presence of H89, with significant displacement of dose-response curves (**, $P < 0.01$, ANOVA; GraphPad Prism). Relaxation was measured as integrated area under the tension curve. Data points represent the mean ± SEM. E, EC_{50} calculated after fitting of idealized dose-response curves using GraphPad Prism software. Rolipram, n = 4; H89 pretreatment and rolipram, n = 4. M_r, Relative molecular mass × 1000.

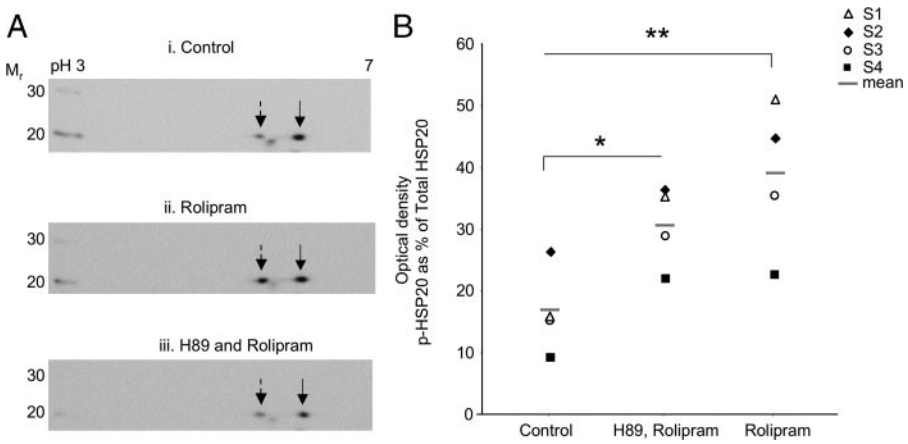

FIG. 4. Changes in phosphorylation of HSP20 in myometrial strips treated with rolipram in the presence and absence of H89. A, Representative 2D immunoblots of HSP20 expression in myometrial strips treated with rolipram in the presence and absence of H89. H89 pretreatment reduced the rolipram-stimulated increase in pHSP20 (*dashed arrow*). B, Densitometry revealed a significant increase in pHSP20 after rolipram (**, $P < 0.01$). There was a trend toward reduced HSP20 phosphorylation by rolipram in the presence of H89 (*, $P < 0.05$) compared with matched controls. Individual data points for each muscle strip shown. *Black arrow*, Unphosphorylated HSP20; S, sample; M_r, relative molecular mass × 1000.

HSP20 coimmunoprecipitates with HSP27 and α-SMA in human myometrial smooth muscle

HSP20 and HSP27 are directly implicated in modulating actin filaments in other cell types. To determine protein binding partners of HSP20 in myometrium, coimmunoprecipitation studies were performed. Protein was extracted from NL myometrium frozen after cesarean section (representing the *in vivo* state), and from control strips after organ bath experiments. Extracts were immunoprecipitated (IP) with anti-total HSP20 antibody and resolved by 1D SDS-PAGE. Immunoblotting of IP protein with anti-total HSP20 antibody revealed two bands: one of molecular mass of approximately 21 kDa, consistent with the presence of HSP20 protein in the IP protein extracts; the other at approximately 42 kDa (Fig. 5). This band was absent from the negative control and may represent HSP20 dimers. Additionally, the 42-kDa band was not observed in samples extracted with the denaturing lysis buffer for 1D SDS-PAGE and immunoblotting (data not shown) but is evident in samples extracted with the less stringent Nonidet P-40 buffer used for immunoprecipitation studies to maintain protein-protein interactions. A specific band of about 40 kDa was also noted in coimmunoprecipitation studies by Brophy and colleagues (31), although this was attributed to the presence of IgG light chains. This appears unlikely, because no similar band was seen in the negative control, and the molecular mass of IgG light chains is reported as approximately 25 kDa (Fig. 5) (32). Moreover, the original purification and identification of HSP20 from human skeletal muscle similarly demonstrated a specific approximately 42-kDa band, present only in those samples resolved by 1D SDS-PAGE in the absence of reducing agent (12).

Probing HSP20 immunoprecipitates with anti-total HSP27 antibody revealed a specific band at approximately 27 kDa, indicating an interaction between HSP20 and HSP27 (Fig. 5). Similarly, a specific band at 44 kDa was detected in immunoprecipitates probed with α-SMA antibody. There appeared to be a stronger association between HSP20 and α-SMA in NL myometrial (*in vivo*) samples, with lower intensity of bands observed in protein obtained after organ bath experiments (*in vitro*) (Fig. 5).

HSP20 in term NL and L myometria

Immunoblotting after 1D SDS-PAGE was performed to examine total HSP20 expression in NL and L myometria, and bands were standardized to α-SMA (Fig. 6A). Total HSP20 abundance did not change between term NL (n = 13) and L (n = 10) samples (Fig. 6B). To examine HSP20 phosphorylation in term NL (n = 4) and L (n = 4) myometria, protein extracts of samples frozen after cesarean section were separated by 2D SDS-PAGE and immunoblotting performed (Fig. 6C). No change in pHSP20 levels was detected (Fig. 6D).

To investigate the cellular localization of HSP20, coimmunofluorescence was performed. In NL and L myometria, staining for HSP20 revealed the protein was located in the perinuclear and cytoplasmic regions (Fig. 6E). Low levels of colocalization were observed between HSP20 and α-SMA in NL myometria. In L samples, modest colocalization between HSP20 and α-SMA was evident in the cytoplasm of some cells (Fig. 6E).

Discussion

sHSPs have a critical role in regulating the actin filament, with phosphorylated HSP27 promoting contraction (33, 34), whereas pHSP20 produces relaxation of vascular muscle (25, 26, 28). We document for the first time the presence of HSP20 in human pregnant myometria and provide evidence that HSP20 phosphorylation occurs specifically during cyclic-nucleotide-mediated myometrial relaxation. Furthermore, we demonstrate an association of HSP20 with the contractile apparatus as well as the actin binding protein HSP27.

pHSP20 is consistently associated with cyclic-nucleotide-mediated inhibition of agonist-induced contraction in vascular muscle (11, 19, 20, 22). We demonstrate that HSP20 is phosphorylated in myometrial tissue during sustained cAMP-mediated relaxation. Forskolin and the PDE inhibitor rolipram produced significant increases in HSP20 phosphorylation, with a 2.6- and 2.1-fold elevation, respectively (Fig. 2, D and E). This was associated with a marked reduction in spontaneous contractions (Fig. 1). A similar 3-fold increase in pHSP20 (isoform pI 5.9) has been reported during forskolin-mediated relaxation of bovine carotid artery (11). The increase in phosphorylation was seen after treatment with a single dose of forskolin (10^{-5} M for 10 min) in explant studies (data not shown) and after application of cumulative doses of forskolin or rolipram to organ bath experiments, with typical treatment durations of 120 min. This concurs with vascular muscle studies, where prolonged relaxation by forskolin or nitric oxide donor glyceryl trinitrate similarly caused increased pHSP20 (22). In carotid artery, cyclic-nu-

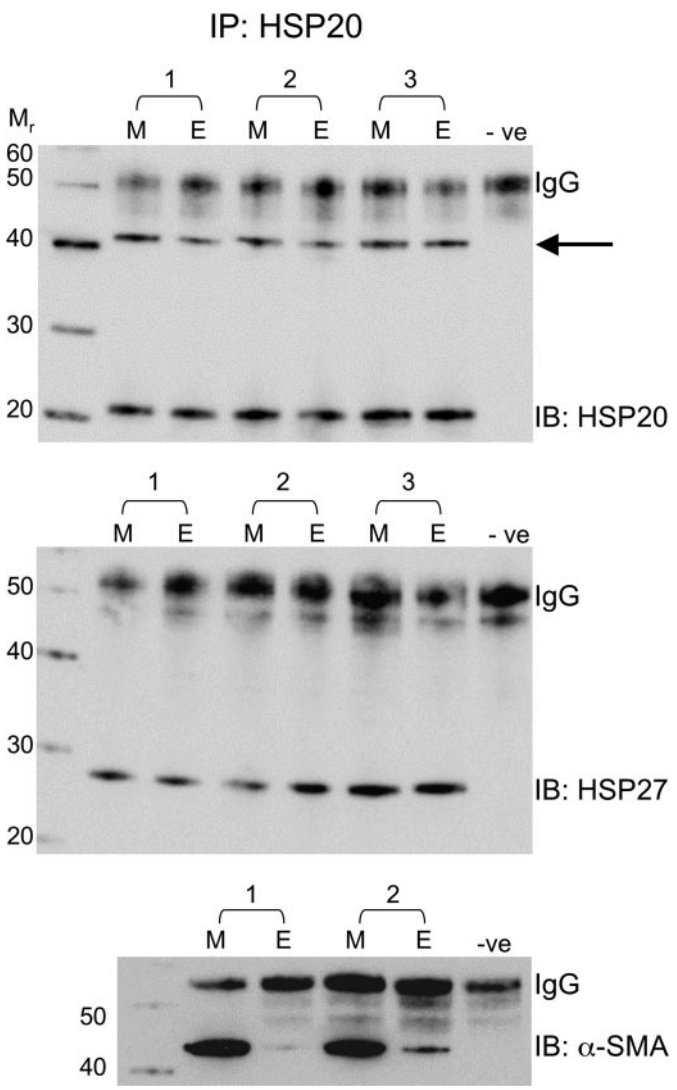

FIG. 5. Interaction of HSP20 with HSP27 and α-SMA in pregnant term myometria. Myometrial protein extracts obtained from samples immediately frozen after lower segment cesarean section (M) or after myometrial organ bath experiments (E) were immunoprecipitated (IP) using rabbit anti-total HSP20 antibody. A negative control (-ve) of pooled myometrial protein was immunoprecipitated with normal rabbit IgG antibody. IP protein extracts were resolved by 1D SDS-PAGE and transferred to nitrocellulose. Immunoblotting (IB) was performed using antibodies for total HSP20, total HSP27, and α-SMA. A second band detected by total HSP20 antibody was also seen at approximately 42 kDa (*arrow*). A band was seen in all samples at approximately 52 kDa, representing IgG heavy chains.

cleotide-induced increases in pHSP20 were not detected at 1 min during the initial rapid relaxation transient but were seen at 2 min and maintained at 45 min, with HSP20 dephosphorylation occurring before redevelopment of force (22). Currently, no information is available regarding phosphatases causing HSP20 dephosphorylation.

HSP20 protein immunoprecipitated from carotid artery is phosphorylated *in vitro* by incubation with PKA catalytic subunits (11). Pretreatment with PKA inhibitor H89 significantly attenuated rolipram-induced relaxation (Fig. 3). pHSP20 induced by rolipram was reduced in the presence of H89 (Fig. 4), providing evidence for a functional myometrial cAMP/PKA pathway phosphorylating HSP20. Additionally, noncyclic-nucleotide-mediated myometrial relaxation induced by nifedipine caused no alteration in pHSP20 (Fig. 2, C and F) while potently inhibiting contractions (Fig. 1). Hence, pHSP20 is not necessary to cause myometrial relaxation, but given the effect of phosphopeptide HSP20 analogs in other muscles, this suggests pHSP20 is sufficient to cause smooth muscle relaxation.

Transducible phosphorylated full-length HSP20 or shorter phosphopeptide analogs directly inhibit agonist-induced vascular contraction (25, 26, 28). The molecular mechanism by which pHSP20 produces smooth muscle relaxation is debated. Our coimmunoprecipitation studies show HSP20 specifically associates with α-SMA and HSP27 (Fig. 5). The association of HSP20 with HSP27 concurs with findings in skeletal muscle (12, 35). It remains controversial whether HSP20 directly binds to α-SMA (36), but our findings are consistent with reports demonstrating a similar relationship with α-SMA in vascular muscle (31, 37). Thus, changes in HSP20 phosphorylation may directly or indirectly (through HSP27) alter the actin filament to modify force.

Our coimmunofluorescence studies reveal that HSP20 is diffusely distributed through the perinuclear area and cytoplasm. Although low levels of colocalization are seen between HSP20 and α-SMA in NL myometria, in L samples, HSP20 is moderately colocalized in the cytoplasm with α-SMA (Fig. 6E). HSP20 also partially colocalizes with actin in vascular muscle (38). Interestingly, cosedimentation studies have reported that unphosphorylated HSP20 is predominantly associated with F-actin, whereas pHSP20 is dissociated from the cytoskeleton (37); however, opposing findings were noted by Rembold *et al.* (19). The degree of colocalization between HSP20 and α-SMA was less than that observed between HSP27 and α-SMA in myometrium (18). This is consistent with the theory that pHSP20 induces relaxation through alteration of the actin filament indirectly, via its association with HSP27 or other proteins (39, 40), rather than directly binding to and inhibiting actin (2, 41). HSP27 regulates F-actin structure (16, 42). A recent hypothesis is that pHSP20 dimers interact with scaffold protein 14-3-3γ, to displace phosphorylated cofilin from 14-3-3γ, thereby allowing the subsequently dephosphorylated cofilin to depolymerize F-actin (27, 43).

Studies in rat myometrium report total HSP20 protein remained at high levels until midgestation, with subsequent decline thereafter. Lowest levels were noted at labor, with a marked reduction in expression in immunofluorescence studies (29). We found total HSP20 protein was unchanged in a larger cohort of term NL and L myometria (Fig. 6, A and B), with no alteration in pHSP20 at term (Fig. 6, C and D). This is not unexpected given our findings that higher levels of pHSP20 are associated with sustained cyclic-nucleotide-mediated relaxation (Figs. 1 and 2). Moreover, myometrial cyclic-nucleotide-dependent pathways are hypothesized to be down-regulated in term pregnant uteri (44–46), shifting from relaxant pathways promoting quiescence to dominance of contractile pathways to generate powerful contractions for delivery. Our findings, together with the gestational changes of HSP20 observed in rat myometrium, highlight a likely function for HSP20 as a mediator of myometrial quiescence

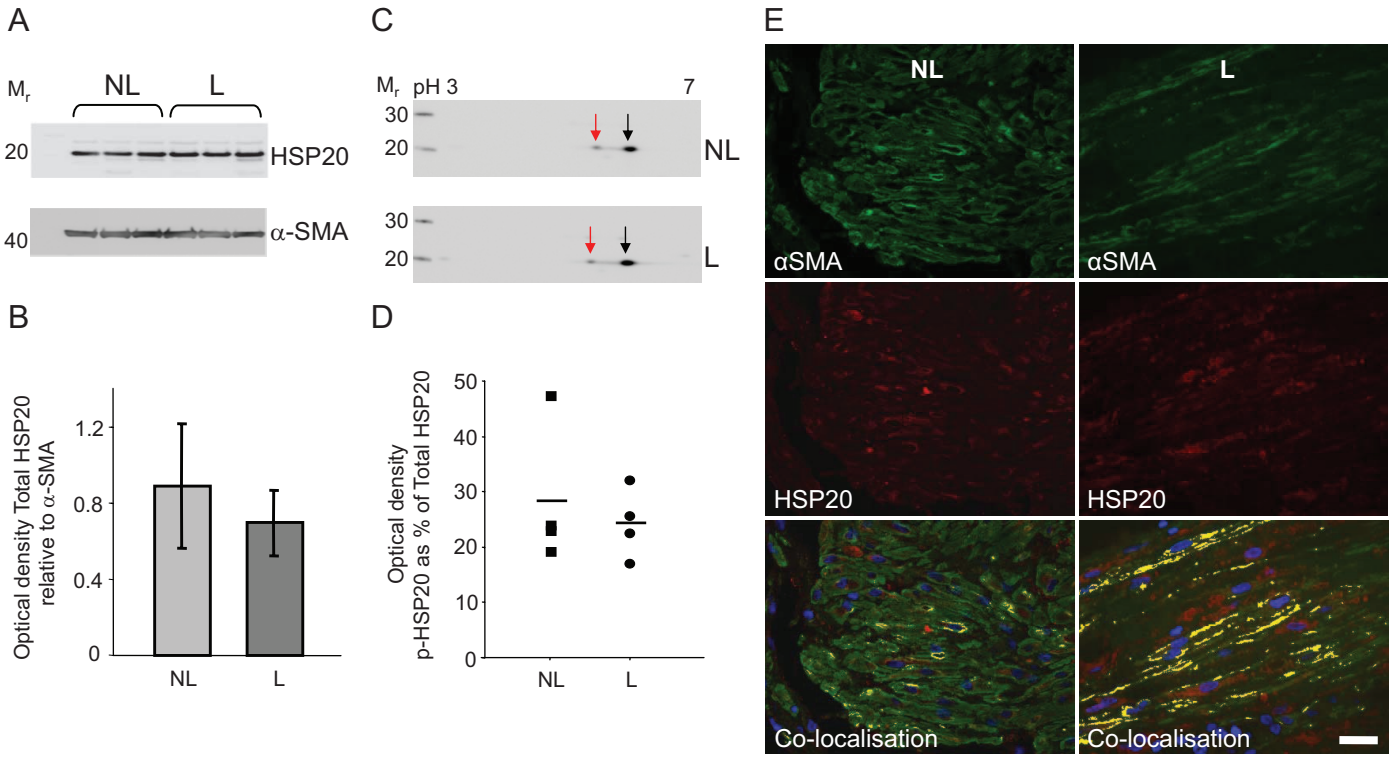

FIG. 6. HSP20 expression in NL and L myometria. A, Representative 1D immunoblot of total HSP20 abundance in NL (n = 13) and L (n = 10) myometria. B, Densitometric analysis showed no change in total HSP20 with labor onset. Band intensity was standardized to α-SMA. C, Representative 2D immunoblot of HSP20 in NL (n = 4) and L (n = 4) myometria. D, Densitometric analysis showed no change in pHSP20 with labor onset. Individual data points for each sample shown. E, Colocalization of HSP20 with α-SMA in NL (n = 5) and L (n = 5) myometrial sections. Colocalization masks that highlight regions of costaining were generated as described in *Materials and Methods*. Low levels of colocalization (*yellow*) were detected between HSP20 (*red*) and α-SMA (*green*) in NL sections, whereas in L sections, HSP20 showed moderate colocalization with α-SMA along fibril actin bundles. Nuclei are shown in *blue*. *Scale bar*, 20 μm. *Red arrow*, pHSP20; *black arrow*, unphosphorylated HSP20; *black bar*, mean; M_r, relative molecular mass × 1000.

and are consistent with the proposed role of pHSP20 as an important regulator of smooth muscle contractility.

Thus, we provide biochemical, structural, and functional evidence of an additional signaling pathway culminating in phosphorylation of a novel myometrial protein, HSP20, associated with inhibition of spontaneous contractions. Consistent with studies in other muscles, myometrial HSP20 is phosphorylated *in vitro* by agents elevating cAMP. Myometrial HSP20 is associated with α-SMA and HSP27. These data support a new role for pHSP20 in modulating myometrial relaxation through interaction with actin. pHSP20 may contribute to myometrial quiescence and represents an important target for future tocolytic therapy.

Acknowledgments

We are grateful to T. Engel, T. Finnegan, Dr. George Yeo, and Dr. Kenneth Kwek as well as the obstetrics staff at John Hunter Hospital and KK Women's and Children's Hospital for their assistance in recruiting our patients. We thank Dr. R. F. Thorne (Cancer Research Unit, University of Newcastle, Australia) for his advice regarding the immunofluorescence studies.

Received April 25, 2008. Accepted August 15, 2008.

Address all correspondence and requests for reprints to: Dr. Elisa Tyson, Department of Endocrinology, Mothers and Babies Research Centre, John Hunter Hospital, Lookout Road, New Lambton Heights, Newcastle 2305, Australia. E-mail: elisa.tyson@studentmail.newcastle.edu.au.

This work was supported by National Health and Medical Research Council of Australia Project Grant. E.K.T. was supported by a National Health and Medical Research Council of Australia Postgraduate Scholarship.

Disclosure Statement: E.K.T., D.A.M., E.C., and M.R. have nothing to declare. R.S. consults for Eurodiagnostica.

References

1. **Tang DD, Gunst SJ** 2004 The small GTPase Cdc42 regulates actin polymerization and tension development during contractile stimulation of smooth muscle. J Biol Chem 279:51722–51728
2. **Meeks MK, Ripley ML, Jin Z, Rembold CM** 2005 Heat shock protein 20-mediated force suppression in forskolin-relaxed swine carotid artery. Am J Physiol Cell Physiol 288:C633–C639
3. **Mehta D, Gunst SJ** 1999 Actin polymerization stimulated by contractile activation regulates force development in canine tracheal smooth muscle. J Physiol 519:829–840
4. **Tseng S, Kim R, Kim T, Morgan KG, Hai CM** 1997 F-actin disruption attenuates agonist-induced [Ca^{2+}], myosin phosphorylation, and force in smooth muscle. Am J Physiol Cell Physiol 272:C1960–C1967
5. **Obara K, Yabu H** 1994 Effect of cytochalasin B on intestinal smooth muscle cells. Eur J Pharmacol 255:139–147
6. **Shaw L, Ahmed S, Austin C, Taggart MJ** 2003 Inhibitors of actin filament polymerisation attenuate force but not global intracellular calcium in isolated pressurised resistance arteries. J Vasc Res 40:1–10
7. **Lopez Bernal A** 2007 The regulation of uterine relaxation. Semin Cell Dev Biol 18:340–347
8. **Barany M, Barany K** 1993 Dissociation of relaxation and myosin light chain dephosphorylation in porcine uterine muscle. Arch Biochem Biophys 305: 202–204
9. **McDaniel NL, Chen XL, Singer HA, Murphy RA, Rembold CM** 1992 Nitrovasodilators relax arterial smooth muscle by decreasing [Ca^{2+}]$_i$ and un-

coupling stress from myosin phosphorylation. Am J Physiol Cell Physiol 263:C461–C467
10. **Nishimura J, van Breemen C** 1989 Direct regulation of smooth muscle contractile elements by second messengers. Biochem Biophys Res Commun 163: 929–935
11. **Beall AC, Kato K, Goldenring JR, Rasmussen H, Brophy CM** 1997 Cyclic nucleotide-dependent vasorelaxation is associated with the phosphorylation of a small heat shock-related protein. J Biol Chem 272:11283–11287
12. **Kato K, Goto S, Inaguma Y, Hasegawa K, Morishita R, Asano T** 1994 Purification and characterization of a 20-kDa protein that is highly homologous to αB crystallin. J Biol Chem 269:15302–15309
13. **Arrigo AP, Suhan JP, Welch WJ** 1988 Dynamic changes in the structure and intracellular locale of the mammalian low-molecular-weight heat shock protein. Mol Cell Biol 8:5059–5071
14. **Lavoie J, Lambert H, Hickey E, Weber L, Landry J** 1995 Modulation of cellular thermoresistance and actin filament stability accompanies phosphorylation-induced changes in the oligomeric structure of heat shock protein 27. Mol Cell Biol 15:505–516
15. **Rogalla T, Ehrnsperger M, Preville X, Kotlyarov A, Lutsch G, Ducasse C, Paul C, Wieske M, Arrigo AP, Buchner J, Gaestel M** 1999 Regulation of Hsp27 oligomerization, chaperone function, and protective activity against oxidative stress/tumor necrosis factor α by phosphorylation. J Biol Chem 274:18947–18956
16. **Lavoie J, Hickey E, Weber L, Landry J** 1993 Modulation of actin microfilament dynamics and fluid phase pinocytosis by phosphorylation of heat shock protein 27. J Biol Chem 268:24210–24214
17. **Landry J, Huot J** 1995 Modulation of actin dynamics during stress and physiological stimulation by a signaling pathway involving p38 MAP kinase and heat-shock protein 27. Biochem Cell Biol 73:703–707
18. **MacIntyre DA, Tyson EK, Read M, Smith R, Yeo G, Kwek K, Chan EC** 2008 Contraction in human myometrium is associated with changes in small heat shock proteins. Endocrinology 149:245–252
19. **Rembold CM, Foster DB, Strauss JD, Wingard CJ, Van Eyk JE** 2000 cGMP-mediated phosphorylation of heat shock protein 20 may cause smooth muscle relaxation without myosin light chain dephosphorylation in swine carotid artery. J Physiol 524:865–878
20. **Beall A, Bagwell D, Woodrum D, Stoming TA, Kato K, Suzuki A, Rasmussen H, Brophy CM** 1999 The small heat shock-related protein, HSP20, is phosphorylated on serine 16 during cyclic nucleotide-dependent relaxation. J Biol Chem 274:11344–11351
21. **Woodrum DA, Brophy CM, Wingard CJ, Beall A, Rasmussen H** 1999 Phosphorylation events associated with cyclic nucleotide dependent inhibition of smooth muscle contraction. Am J Physiol Heart Circ Physiol 277:H931–H939
22. **Rembold CM, O'Connor M, Clarkson M, Wardle RL, Murphy RA** 2001 Signal transduction in smooth muscle selected contribution: HSP20 phosphorylation in nitroglycerin- and forskolin-induced sustained reductions in swine carotid media tone. J Appl Physiol 91:1460–1466
23. **Bergh CM, Brophy CM, Dransfield DT, Lincoln T, Goldenring JR, Rasmussen H** 1995 Impaired cyclic nucleotide-dependent vasorelaxation in human umbilical artery smooth muscle. Am J Physiol Heart Circ Physiol 268:H202–H212
24. **Brophy C, Beall A, Lamb S, Dickinson M, Ware D** 1997 Small heat shock proteins and vasospasm in human umbilical artery smooth muscle. Biol Reprod 57:1354–1359
25. **Woodrum D, Pipkin W, Tessier D, Komalavilas P, Brophy CM** 2003 Phosphorylation of the heat shock-related protein, HSP20, mediates cyclic nucleotide-dependent relaxation. J Vasc Surg 37:874–881
26. **Tessier DJ, Komalavilas P, Liu B, Kent CK, Thresher JS, Dreiza CM, Panitch A, Joshi L, Furnish E, Stone W, Fowl R, Brophy CM** 2004 Transduction of peptide analogs of the small heat shock-related protein HSP20 inhibits intimal hyperplasia. J Vasc Surg 40:106–114
27. **Dreiza CM, Brophy CM, Komalavilas P, Furnish EJ, Joshi L, Pallero MA, Murphy-Ullrich JE, Von Rechenberg M, Ho YS, Richardson B, Xu N, Zhen Y, Peltier JM, Panitch A** 2005 Transducible heat shock protein 20 (HSP20) phosphopeptide alters cytoskeletal dynamics. FASEB J 19:261–263
28. **Flynn CR, Brophy CM, Furnish EJ, Komalavilas P, Tessier D, Thresher J, Joshi L** 2005 Transduction of phosphorylated heat shock-related protein 20, HSP20, prevents vasospasm of human umbilical artery smooth muscle. J Appl Physiol 98:1836–1845
29. **Cross BE, O'Dea HM, MacPhee DJ** 2007 Expression of small heat shock-related protein 20 (HSP20) in rat myometrium is markedly decreased during late pregnancy and labour. Reproduction 133:807–817
30. **Mehats C, Tanguy G, Paris B, Robert B, Pernin N, Ferre F, Leroy MJ** 2000 Pregnancy induces a modulation of the cAMP phosphodiesterase 4-conformers ratio in human myometrium: consequences for the utero-relaxant effect of PDE4-selective inhibitors. J Pharmacol Exp Ther 292:817–823
31. **Tessier DJ, Komalavilas P, Panitch A, Joshi L, Brophy CM** 2003 The small heat shock protein (HSP) 20 is dynamically associated with the actin cross-linking protein actinin. J Surg Res 111:152–157
32. **Weiner JA, Chun J** 1997 Maternally derived immunoglobulin light chain is present in the fetal mammalian CNS. J Neurosci 17:3148–3156
33. **Yamboliev IA, Hedges JC, Mutnick JL-M, Adam LP, Gerthoffer WT** 2000 Evidence for modulation of smooth muscle force by the p38 MAP kinase/HSP27 pathway. Am J Physiol Heart Circ Physiol 278:H1899–H1907
34. **Bitar KN, Kaminski MS, Hailat N, Cease KB, Strahler JR** 1991 Hsp27 is a mediator of sustained smooth muscle contraction in response to bombesin. Biochem Biophys Res Commun 181:1192–1200
35. **Kato K, Shinohara H, Goto S, Inaguma Y, Morishita R, Asano T** 1992 Copurification of small heat shock protein with αB crystallin from human skeletal muscle. J Biol Chem 267:7718–7725
36. **Bukach OV, Marston SB, Gusev NB** 2005 Small heat shock protein with apparent molecular mass 20 kDa (Hsp20, HspB6) is not a genuine actin-binding protein. J Muscle Res Cell Motil 26:175–181
37. **Brophy CM, Lamb S, Graham A** 1999 The small heat shock-related protein-20 is an actin-associated protein. J Vasc Surg 29:326–333
38. **Rembold C, Zhang E** 2001 Localization of heat shock protein 20 in swine carotid artery. BMC Physiol 1:10
39. **Brophy CM** 2000 The dynamic regulation of blood vessel caliber. J Vasc Surg 31:391–395
40. **Fuchs LC, Giulumian AD, Knoepp L, Pipkin W, Dickinson M, Hayles C, Brophy C** 2000 Stress causes decrease in vascular relaxation linked with altered phosphorylation of heat shock proteins. Am J Physiol Regul Integr Comp Physiol 279:R492–R498
41. **Rembold CM** 2007 Force suppression and the crossbridge cycle in swine carotid artery. Am J Physiol Cell Physiol 293:C1003–C1009
42. **Benndorf R, Hayess K, Ryazantsev S, Wieske M, Behlke J, Lutsch G** 1994 Phosphorylation and supramolecular organization of murine small heat shock protein HSP25 abolish its actin polymerization-inhibiting activity. J Biol Chem 269:20780–20784
43. **Chernik IS, Seit-Nebi AS, Marston SB, Gusev NB** 2007 Small heat shock protein Hsp20 (HspB6) as a partner of 14-3-3γ. Mol Cell Biochem 295:9–17
44. **Grammatopoulos D, Stirrat G, Williams S, Hillhouse E** 1996 The biological activity of the corticotropin-releasing hormone receptor-adenylate cyclase complex in human myometrium is reduced at the end of pregnancy. J Clin Endocrinol Metab 81:745–751
45. **Litime M, Pointis G, Breuiller M, Cabrol D, Ferre F** 1989 Disappearance of β-adrenergic response of human myometrial adenylate cyclase at the end of pregnancy. J Clin Endocrinol Metab 69:1–6
46. **Europe-Finner G, Phaneuf S, Tolkovsky A, Watson S, Lopez Bernal A** 1994 Down-regulation of G αs in human myometrium in term and preterm labor: a mechanism for parturition. J Clin Endocrinol Metab 79:1835–1839

***Endocrinology* is published monthly by The Endocrine Society (http://www.endo-society.org), the foremost professional society serving the endocrine community.**